3D Process-Oriented Gravity Modelling applied north of 49ºS on theArgentine continental margin

Ana C. Pedraza De Marchi[1,2], Marta E. Ghidella[3], Claudia N. Tocho[1,4]

[1]Universidad Nacional de La Plata, Facultad de Ciencias Astronómicas y Geofísicas, La Plata, 1900, Argentina
[2]CONICET, National Council of Scientific and Technical Research, Argentina
[3]Instituto Antártico Argentino, Buenos Aires, C1064AAF, Argentina
[4]Consejo de Investigaciones Científicas de la Provincia de Buenos Aires

Correspondence to: Ana C. Pedraza De Marchi (cpedrazadm@fcaglp.unlp.edu.ar)

Abstract. The Process-Oriented Gravity Modelling (POGM) technique represents a useful way to distinguish the contribution that different geological processes make to the observed gravity in passive margins. The POGM is an innovative gravity modelling approach that can give us information about the role that processes such as sedimentation and magmatic underplating, together with their loading effects, may play in the evolution of a margin. In this work, the POGM methodology has been applied with in a 2D and 3D approach. 2D profiles spaced every one arc-minute in the area of the Argentine continental margin, between 38.5ºS and 49ºS latitude and 64ºW and 50ºW longitude, were used to generate the latter.

The 3D POGM was also solved and the result was compared with that obtained from 2D profiles. The comparison with the observed anomaly, using the 3D approach from 2D profiles gave results with enhanced resolution.

The best fit between the calculated and observed gravity anomaly is given by an effective elastic thickness of 15 km. A cortical thickness map obtained as a result of the POGM calculations shows basin areas characterized by a thinned crust and a structural variation where the continental-oceanic boundary (COB) could be indicated. Besides, results of POGM allow us to detect an alignment between the Valdés and Rawson basins and possibly a third basin as a probable aulacogen. A stretching factor analysis shows that in these basins a stretching period existed but it did not reach the stage of oceanic crust formation. A strong positive residue in the Colorado basin is shown by the flexural isostatic anomaly, suggesting that the basin may continue in subsidence.

1 Introduction

Gravity interpretation studies generally are initiated by estimating preliminary source in depth and density contrast. These estimates are followed by more comprehensive analysis that includes forward modelling using trial-and-error inversion

methods or inverse modelling, where more unknown can be estimated (Hinze et al., 2013.). This traditional treatment can be called "static" modelling approach to gravity anomaly interpretation. On the other hand, gravity anomalies can be calculated considering the results of all processes that have shaped in through time, specifically to continental margins. These processes are rifting, sedimentation and magmatism (Watts and Fairhead, 1999).

One of the most distinctive geophysical features of rifted continental margins is the free-air gravity edge-effect anomaly. In simple terms this effect is composed by a "high" that is correlated with the outer shelf and a "low", associated with slope and rise regions and can be considered as the signature of gravity of passive margins. Usually, the edge-effect is interpreted as the juxtaposition of the thick continental crust and the thin oceanic crust. The anomaly can be explained by a model in which the continent-ocean transition is located in the region of the present-day shelf break, but it appears to be sensitive to the location of the transition. The edge- effect can change abruptly depending on the relative position of the transition and the shelf break (Watts and Fairhead, 1999).

While some margins display the "typical" edge-effect of a similar amplitude and landward high and seaward low wavelength, others zones depart substantially from the expected effect. To better understand the origin of these edge-effect variations, the gravity anomaly has to be computed and associated with different processes occurring in the margins, such as sedimentation and magmatic underplating (Watts and Fairhead, 1999). To gain insight from these gravity anomalies a process oriented approach (POGM) to gravity modelling was used instead of convectional static models. It combines the backstripping technique (Stewart and Watts, 2000; Watts and Stewart, 1998) with gravity modelling techniques. The backstripping is a quantitative technique based on the removal of basement load applied under the hypothesis of Airy or flexural isostasy. Therefore, it is assumed that the load of the crust caused by water and sediment is known. With the backstripping technique the basement depth in the absence of sediment can be estimated, i.e. the palaeo-bathymetry at the time of rifting. This has been calculated considering all the sedimentary deposit as a single event with an average density. In the case of flexural backstripping, an appropriate parameter in the wavenumber domain is determined. This parameter modifies the Airy response and gives the flexure (Watts, 2001).

POGM uses the seismic information of the sediment thickness and the present volcanism (e.g., Seaward Dipping Reflectors [SDRs] and magmatic underplating) of the current margin to estimate the gravity anomaly associated with processes like rifting, sedimentation and magmatism. The objective of POGM is to discriminate the contribution that different processes give to the observed anomaly and the goal of backstripping is to determine the geometry at the time of rifting. The base of the sedimentary deposit considered in the backstripping corresponds to the seismic reflector denominated in the literature as *break-up unconformity.*

The POGM sequence can be summarised as follows:

(1) Backstripping is applied to the sediment load to determine the basement at the time of rifting. The effective elastic thickness (T_e) is a measure of the resistance to vertical deformation of the lithosphere or flexural rigidity, significant differences exist between the T_e structure of oceanic and continental lithosphere.

(2) The stretching factor β is calculated using Airy assumptions to restore the geometry of the Moho at the time of rifting.

(3) Gravity modelling (POGM):

3.1) the gravity anomaly associated with the rift is estimated. For most margins, this anomaly shows the typical edge effect with a high on the continental platform and a low in the slope region and for others, it reveals complexities that do not follow this pattern (Watts, 1999).

3.2) the sediment loading of the margin is restored and the flexure of the basement (same as that in the Moho) is calculated, using the elastic parameter T_e from step 1.

3.3) the anomaly associated with the sedimentary process is calculated, the sediment loading, the flexure of the basement and the Moho depth are determined. In the sedimentation anomaly, maxima ("highs") are associated with sediments denser than the displaced water and lateral minima ("lows") are associated with the displacement of the relatively lower density of the crust within the denser mantle.

3.4) the sum anomaly is obtained by adding the rift anomaly to the sedimentation anomaly.

(4) Finally, the sum anomaly is compared through root mean square (RMS) to the observed anomaly (considered as the free-air anomaly in this work), which represents the main constraint for the T_e parameter.

The same method, with more elaborated steps, was used in the North Atlantic continental margin (Karner and Watts, 1982), in the Namibia continental margin (Stewart and Watts, 2000) and West Africa (Watts and Stewart, 1997). Details of the methods can be found in these papers also.

The purpose of this paper is to present POGM and backstripping testing results in the area of the Argentine continental margin. Such techniques have not been explored previously in this region and represent a useful way to distinguish the contribution of different geological processes to the observed gravity. These contributions can be analyzed isolatedly as the results of independent events and have the potential to give us clues about the role that geologic processes involved with their loading effect may play in the margin evolution. Besides, here we explored a laborious attempt, 3d from 2d, to improve the interpretation from these innovative anomalies and the preliminary conclusions were extracted from them.

What we present in this paper is the first approach to a more comprehensive study in which a thorough comparison with other geophysical and geological data will be necessary.

2 Geological framework

West Gondwana broke up in Early Cretaceous times and subsequent seafloor spreading resulted in the formation of the South Atlantic Ocean. South America rotated clockwise in relationship with Africa and it took almost 40 Ma (Szatmari, 2000).

The opening of the South Atlantic occurred diachronously, progressing from South to North (Rabinowitz y Labreque, 1979). Its early stage of rifting and opening may be described as a 150–84 Ma old successive northward unzipping of rift zones (Nürenberg and Müller, 1991).

At about 70 million years ago the orientation of the spreading between South America and Africa changed, as seen by the change of the orientation of the Walvis Ridge, and the overall spreading rate slowed down. This probably came along with a major erosional phase which is manifested in the seismic data and may be linked to orogenic processes in the Andes. From that time on, the South Atlantic spreading axis began to migrate westward, away from the Tristan da Cunha hot-spot (Franke, 2013).

Continental breakup and initial seafloor spreading in the South Atlantic were accompanied by extensive transient magmatism as inferred from sill intrusions, flood basalt sequences, voluminous volcanic wedges, and high-velocity lower crust at the present continental margins.

The volcanic characteristic of the Argentine margin and its South African conjugate is revealed by the extensive extrusive manifestations that form the South Atlantic Large Igneous Province. These include the Parana-Etendeka Continental Flood Basalts and the offshore counterpart of extrusive complexes, represented by a voluminous volcanic wedge of seaward dipping reflections (SDRs).SDRs are extended along most of the outer Argentine and its conjugate from the South African margin (Blaich et al, 2009).

Franke et al. (2007) made a detailed investigation report of the outer segment of the margin based on a set of 25,000 km of multichannel seismic data acquired by the German Geological Survey (BGR) in the last 10 years. These data show that the structure of the margin and especially the SDRs vary in architecture, extent and thickness along the margin. Franke et al. (2007) suggest that the location of the SDRs from 60 to 120 km wide was probably episodic, and the spread to the northern areas of the South Atlantic rift is widely developed. Nevertheless different segments along the limited scope of what they call "transfer areas" were distinguished by Franke et al. (2007). Franke et al. (2007) defined four higher transfer zones for the Argentine continental margin. These areas are the fracture zones Malvinas-Falkland, the Colorado, Ventana, and Salado transfer zones. These four transfer zones were recently confirmed on the basis of magnetic and gravity data (Blaich et al., 2009).

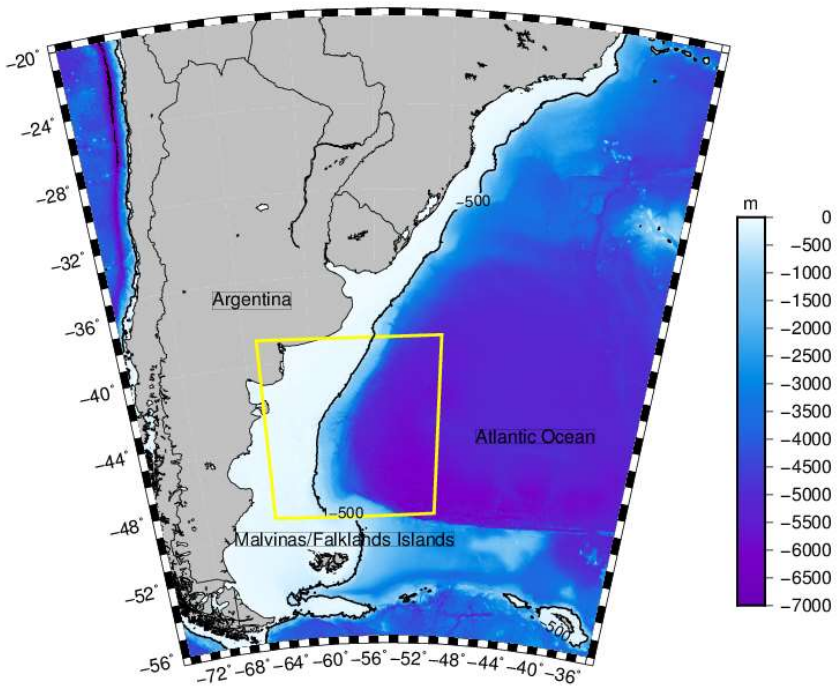

Figure 1: Our study area in the western South Atlantic (yellow rectangle) on top of the bathymetry. The 500 m isobath is plotted as a black line for reference.

3Data and Method

3.1Data Sources

For the development of this workthe area of interest (Figure 1) was selected according to the sedimentary thickness data availability; other data of public domainhave also been used:

3.1.1 Free air gravity anomaly and bathymetry

The ocean surface is an equipotential surface of the terrestrial gravity field (without taking into account the effect of waves, winds, tides and currents). Small elevations and depressions of the geoid (geoid undulation) can be measured by using very precise radars aboard satellites (Sandwell and Smith, 1997). A computational demanding method for converting measurements of geoid elevation (with a variety of different accuracies, spacing paths and data densities) into gravity anomaly grids (or images), have been developed by Sandwell and Smith (1997). In the work by Pedraza et al. (2012) an analysis was conducted by comparing grids of free air gravity anomaly of Sandwell version V16.1, V18.1 and DTU 10 GRA, DNSC08GRA (Andersen et al., 2010) of the Danish Data Center (DTU) with respect to the marine gravity anomalies of different ship track campaigns in the region of the Argentine margin. It was concluded that the advantage of the V18.1, DTU10GRA and DNSC08GRA models against the model V16.1 is due to the use of an accurate geopotential model during

processing and to the different processing techniques used. However, a systematic deviation correlated to the difference between models of the DTU and the shipborne free air gravity anomalies was found latitudinally. Due to this result, the free anomaly grid of the V18.1 version of the Sandwell and Smith was used in this study.

The bathymetry data belongs to the V14.1 version (Sandwell et al., 2001), and is constructed from a combination of sources, such as marine gravity data derived from the Geosat and ERS-1 satellites with a horizontal resolution of 1-12 km.

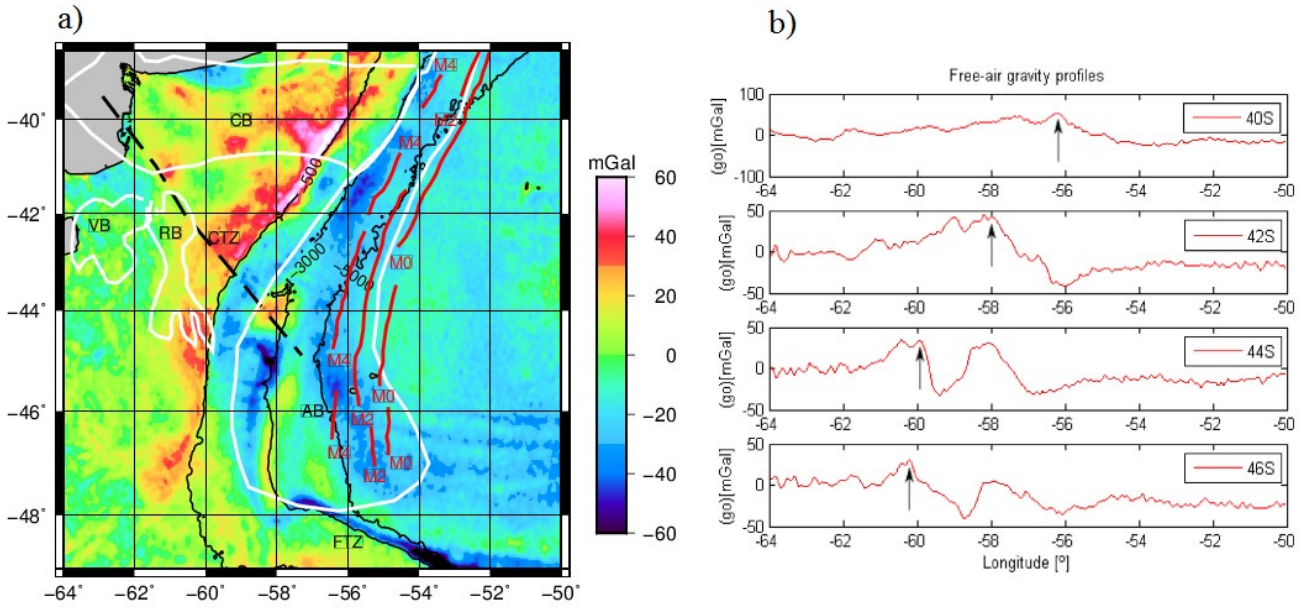

Figure 2: (a) 3D Free-air gravity anomaly. The black dashed line corresponds to the Colorado transfer zone (CTZ) and Malvinas-Falkland transfer zone (FTZ), black solid lines are 500m, 3000m and 5000m isobaths, Mesozoic lineations (Ghidella, 2002) are in red and the Colorado (CB), Rawson (RB), Valdés (VB) and Argentine (AB) basins in white. The Argentine basin was just drawn by hand, and the rest of the basins were digitalized from Franke et al. (2007). (b) Free-air gravity profiles at 40S, 42S, 44S and 46S. The black arrow indicates the "high" of the edge-effect.

The free-air gravity anomalies have very interesting characteristics (Figure 2 a). Eastward the Rawson basin (RB) and to the south of the Colorado discontinuity (CTZ), there is a relative minimum into the gravimetric maximum that borders the slope, and a maximum offshore in the slope region. It seems to indicate a collapse.

Around point of coordinates (44°S, 58°W), which limits to the east with the 3000 m isobath, there is a relative circular gravity maximum located above a sedimentary basin (Neben et al., 2002). It can be identified in the profile (Figure 2b) as a maximum that has not been indicated with the black arrow, the latter represents the edge-effect. Towards the south, there is another relative maximum that forms a band, parallel to 3000 m isobath, which crosses it. This is on the border of the Argentina basin. Positive gravimetric anomalies on sedimentary basins are usually indicative of absence of isostatic compensation of the basin, as occurs in the Salado basin (Introcaso, 1984), which would be under subsidence.

It should also be noted that the orientation of the basins is almost perpendicular to the margin in the north zone and that this changes to the south of CTZ: the basins of Valdés (VB) and Rawson (RB) are representative of a rift sub parallel to the one system of the platform (Ramos, 1996).

It is noticeable that the "high" of the free air edge-effect anomaly fits with the 500m isobaths. It is an interesting characteristic that can be used in a future interpretation of the variation of this effect along the margin in correlation with other geophysical data.

3.1.2 Sedimentary thickness

A compilation of sedimentary thicknesses has been performed using data from several sources and scanned results from published maps (e.g., http://www.martagh.com.ar/mararg/pictr2002/). The first data source in marine zones is from Ludwig et al. (1978) and the terrestrial zones values from the figures of Zambrano and Urien (1970). The second data source is a compilation of geological maps of the Argentine Republic (Caminos and González, 1996) taken by the Naval Hydrographic Service (Parker et al., 1996). The third data source of sedimentary thickness was taken from figure 5 of Neben et al. (2002). These data are in Two-way time (TWT) of the seismic signal in milliseconds, between the seabed and the discordance of rupture ("breakup unconformity") or basement. If the average sound velocity of 2000 m/s is assumed as an approximate estimate of the thickness, similar to Hayes and LaBrecque (1991), a maximum sedimentary thickness of 4000 m is obtained. The equation that relates sedimentary thickness and single transit time (Coscia, 2000) was applied. This is a semi-empirical law arising from the analysis of hundreds of solutions of the sedimentary layers at variable depths in different areas of the Argentine continental margin and was employed to calculate sedimentary thicknesses.

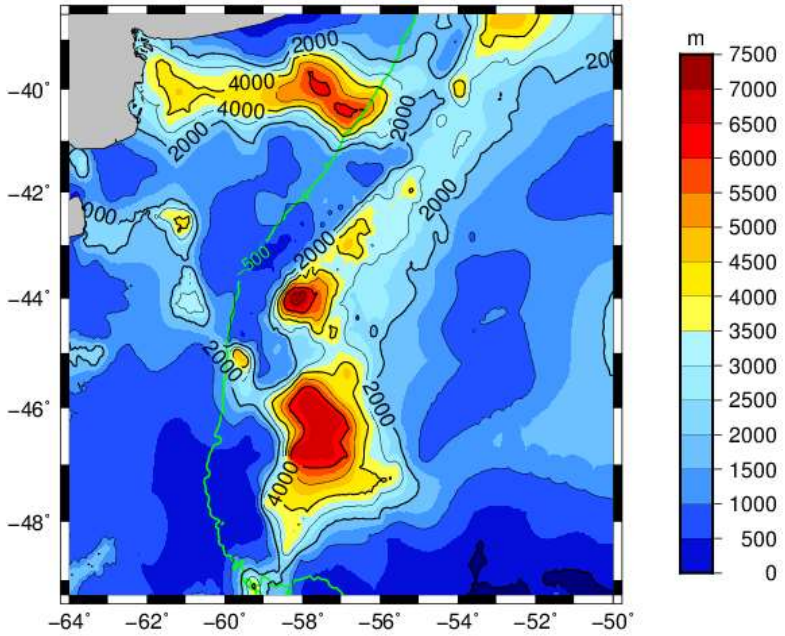

Figure 3: Sedimentary thickness compiled from digitalized the published maps cited in the text. The 500 m isobath is plotted in green line for reference.

Coscia (2000) estimates that the error to determine the sedimentary thickness from this formula is close to 8%. The thickness thus calculated varies between 160 and 7540 m. The resulting map of sedimentary thickness is shown on Figure 3.

The methodology of the POGM technique can be described by the sequence of steps showed in Figure 4. They are:

3.2Method

3.2.1Backstripping

The first step in the sediment backstripping (Watts & Ryan, 1976) is to obtain the total tectonic subsidence (TTS) of the basement. It can be calculated assuming that the load is locally (Airy) or regionally (Flexural) supported (e. g. Watts, 1988).

The backstripping equation is:

$$Y_{\mathrm{i}} = W_{\mathrm{di}} + S^{*}{}_{\mathrm{i}}\left[\frac{\rho_{\mathrm{m}}-\overline{\rho_{\mathrm{si}}}}{\rho_{\mathrm{m}}-\rho_{\mathrm{w}}}\right] - \Delta_{\mathrm{sli}}\frac{\rho_{\mathrm{m}}}{(\rho_{\mathrm{m}}-\rho_{\mathrm{w}})}, \quad (1)$$

where W_{di}, $S^{*}{}_{\mathrm{i}}$and Y_{i} are the water depth, de-compacted sediment thickness and tectonic subsidence of the ithstratigraphic layer, respectively,ρ_{w},ρ_{m}andρ_{si}represent the density of the water, mantle and the de-compacted sediment, respectively, $\Delta_{\mathrm{sli}}$is the high of mean sea-level above (or below) the reference surface.

Disregarding effects of the water loading due to changes in sea level the tectonic subsidence (Y) associated with a sediment thickness S is given by (Eg. &Torné Watts, 1992):

$$\hat{Y}(k) = \hat{S}(k)\Phi(k)\left[\frac{\rho_s-\rho_w}{\rho_m-\rho_{infill}}\right], \quad (2)$$

where the hat in letters represent a 1D or 2D Fourier transform and $k$stands for the number of linear or radial wave, The densities of the mantle and water are: $\rho_m = 3330\,kg/m^3$, $\rho_w = 1030\,kg/m^3$. The average density of the sediment considering a single layer is $\rho_s = 2600\,kg/m^3$.

The flexural parameter is:

$$\Phi(k) = \left[1 + \frac{\mathrm{Dk}^4}{(\rho_m-\rho_{infill})\mathrm{g}}\right]^{-1}, \quad (3)$$

Where g is the average acceleration of gravity$(9.81\ m/s^2)$and D is the flexural rigidity determined (Nm) from the effective elastic thickness T_{e} given by:

$$D = \frac{E\mathrm{T}_e^3}{12(1-\upsilon^2)}, \quad (4)$$

Where E = Young's modulus $(100\ GP_{\mathrm{a}})$ and υ=Poisson radius (0.25). Here we used a T_e range between 0 km to30 km.

Considering the infill density(ρ_{infill})as the water density rather than the sediment density, indicating that the vacant space is filled with water in the flexural unload.

3.2.2 Determination of β

In the second step, the geometry of the rift margin from the known TTS was derived assuming that the thickness of the crust is locally compensated. Thus, the stretching factor, which is the ratio between unstretched and thinned crust thicknesses, depends only on the thickness of the initial crust(T_c) on density of the mantle and on the average density of the crust and the T_e used in the backstripping of sediment loading. In this work the overall POGM, TTS corresponds to the position of the basement in the absence of surface charges (e.g., sedimentary, volcanic) and subsurface charges (e.g., underplating) (Cunha, 2008).

In this step, a paleo-bathymetry at the time of rifting is estimated. Isostatic equilibrium according to Airy with a normal thickness of the crust of 32 km is applied in order to calculate theβparameter. This parameter allows us to find the crust structure and therefore the Moho topography at the time of rifting.

$$\beta = \left[\frac{T_c(\rho_m-\rho_w)}{T_c(\rho_m-\rho_c)-TS(\rho_m-\rho_w)}\right], \quad (5)$$

WhereT_c is a normal thickness crust (32km), *TS* is the backstripping calculated for each T_e, and the density of the crust $is\ \rho_c = 2800\,kg/m^3$.

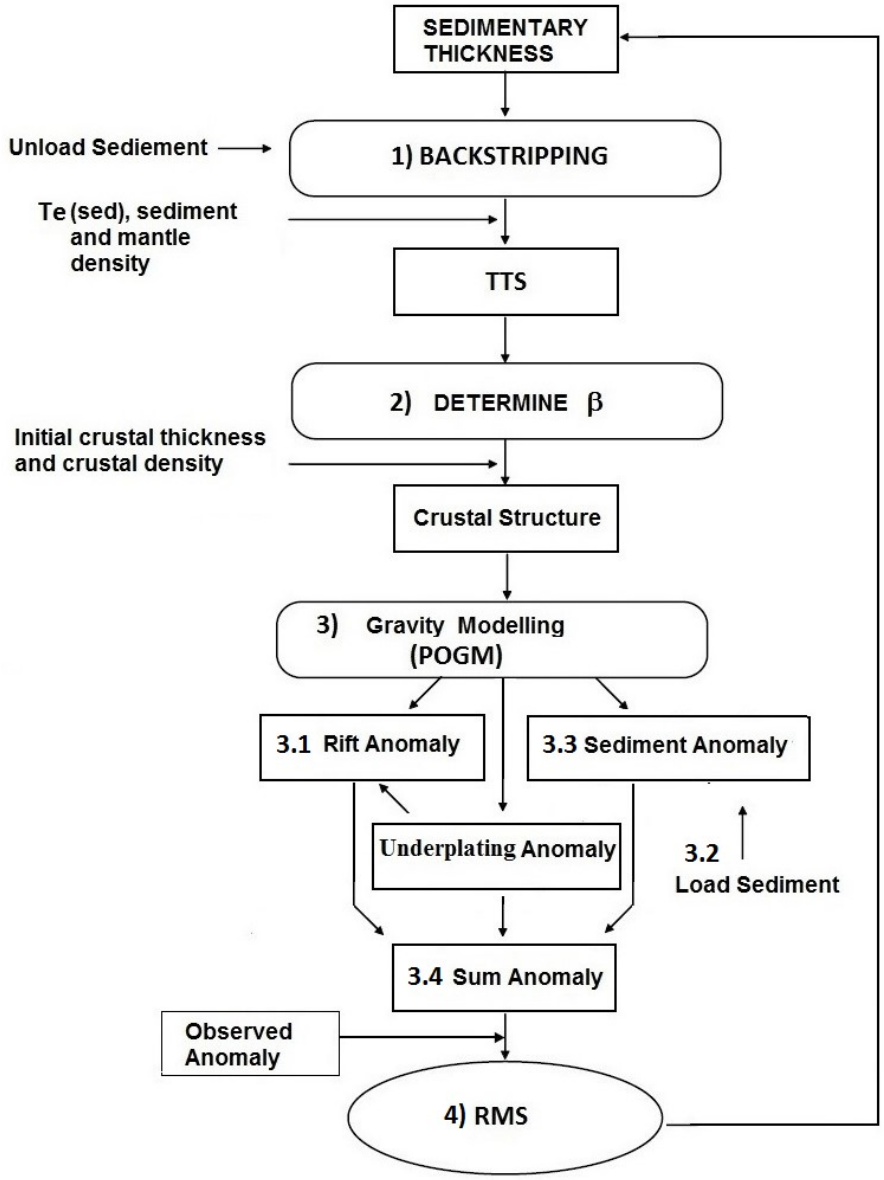

Figure 4: Diagram for implementing the POGM method. Modify from (Stweart et al., 2000)

3.2.3 Gravity modelling

Once the backstripping is finished, the thickness of the crust under extension can be estimated. The main issue is that the true value of the elastic thickness(T_e)is not known to be used in the backstripping of sediments and that the configuration of the crust at the time of rifting can be reset.

The gravity anomaly can be used to constrain (T_e) values.For a rift, it appears to be sensitive to the initial crust structure and processes such as sedimentation, magmatic underplating and erosion.

By calculating the gravity anomaly caused by the initial structure of the rift and the associated with the modifying processes and comparing it with the observed anomaly, a procedure that can restrict the Te values is obtained. Watts and Fairhead(1999) suggested calling this procedure "process-oriented gravity modelling", a technique based on three steps:

a) the gravity anomaly due to backstripping obtained from a water filled basin and its compensation is calculated. This is called the *rift anomaly*.

b) the gravity anomaly due to sediment loading is obtained and its compensation is calculated. This is known as the *sediment anomaly*. The load of the sediment is given by the difference between the backstripping result and the current topography.

c) In the final step the sum anomaly due to the rift and sedimentation is calculated and the observed anomaly on the rift basin is compared.

Continental margins can be segmented with respect to their flexural rigidity, which may partly explain variations in gravity anomalies observed in some margins (e.g., Gabon / Angola; (Watts et al. 1998).

Backstripping and gravity modelling techniques are combined in a process oriented gravity modelling (Watts and Fairhead, 1999, Watts, 2001). Initially, the backstripping technique is applied to profiles allowing to estimate the depth of the basement in the absence of sediment (i.e. palaeo-bathymetry at the time of rifting). This step was calculated taking into account the entire thickness of the sediments without age differentiation.

In the case of flexural backstripping, a relevant parameter is determined in the wavenumber space which modifies the Airy response producing the flexural response resulting from an equivalent equation to equation (6.5) in the Fourier domain.

Seismic information of sedimentary thickness and present volcanic activity (SDRs, underplating, etc.) in the current margin configuration is used by the POGM to estimate the gravity anomaly associated with sedimentation and magmatism processes.

In Watts and Fairhead (1999) there are tests with synthetic profiles that explain what we can expect from the method in each step.

4 Gravity modelling results

Steps 1) to 4) of Figure 4 can be applied to 2D profiles and then extended to the 3D case. First, a 3D field through collecting 2D longitudinal profiles separated by a latitudinal spacing of 1 ' can be approached to keep the same spatial resolution as in the observed data. Then all the equations involved in steps 1) to 4) in 3D can be solved and the result can be compared with the approach from 2D profiles.

4.1 Applying the backtripping to the sediment loading (step 1, Figure 4)

Figure 5 (a) shows the result of the backstripping technique that allows us to visualize an estimate of the palaeo-bathymetry at the time of rifting for the assumptions made and (b) the palaeo Moho. Colorado, Valdés and Rawson basins and their compensation can be identified.

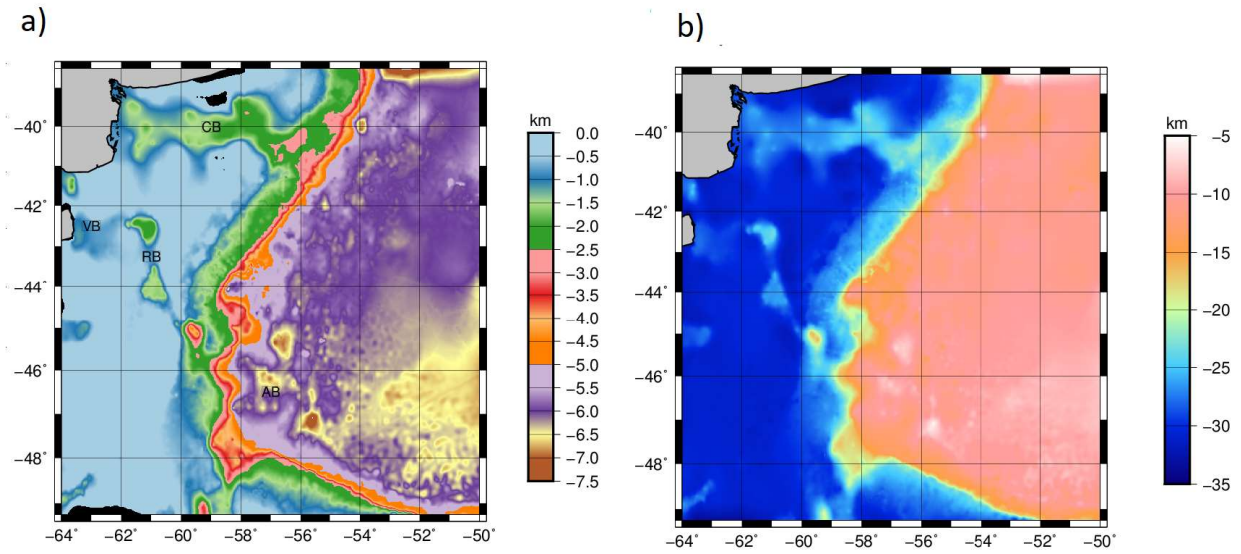

Figure 5: (a) one 3D estimation of the palaeo-bathymetry at the time of rift and (b) of the palaeoMoho, from 2D profile. CB: Colorado basin, VB: Valdés basin and RB Rawson basin.

4.2 Calculating the stretching factor β according to Airy (step 2, Figure 4)

Intracontinental sedimentary basins are typically characterized by a β value of 2.A β value of 5 indicating that the breakup and the generation of new ocean can occur (White et al., 1989).

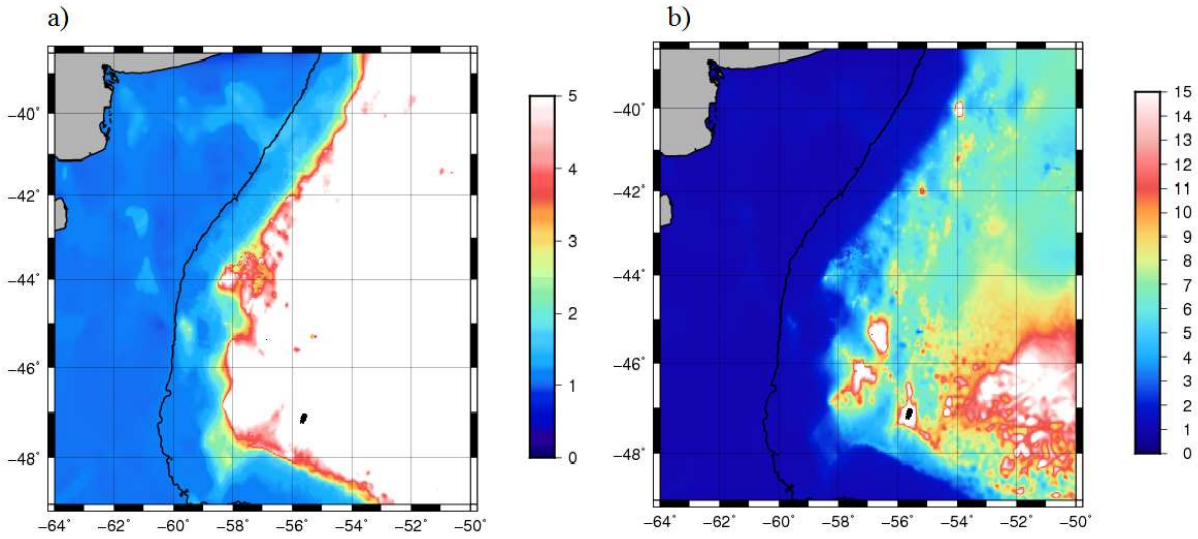

Figure 6: (a) Stretching factor β emphasizing the platform area (b) Stretching factor β in the marine deeper zone. In both figures the 500 m isobath is plotted in black line for reference.

Stretching factors up to about 5 generally represent crust on extension and are present in rifts in evolution. For complete rift processes, with oceanic crust and created ocean basin, they tend to infinity. In our case, the areal distribution in Fig. 6 shows values close to 2 in the Colorado, Valdés and Rawson basins, and in the neighbouring area, the stretching factor is lower, being evidence of the crust shortening while Fig. 5b has the highest values in the deep ocean area, especially in a region to south of 45 ° S. This could represent the fact that the ocean extension created here was higher and faster, consistent with what tectonic models suggested (Moulin et al., 2010, Eagles et al., 2008, Rabinowiz et.al., 1979).

Colorado, Valdés and Rawson basins appear on the map of palaeo-bathymetry at the time of rifting showing a stretching factor greater than the environment (Figure 6a).

4.3 Calculating the crustal thickness (step Crustal Structure, Figure 4)

Figure 7 shows the spatial distribution of the crustal thickness that is derivated from POGM calculations; it is characterized by a thinned crust in basins areas (Figure 2) and a strong gradient near to the 3000m isobath. We have digitized the interface of the basement and Moho from an interpreted refraction profile by Franke et al. (2002) and the comparison with the same profile was made from the map (Figure7a). The major discrepancies between both profiles (Figure7b) are in the zone of the presence of a high-velocity body (59w to 56w) with dimension of approximately 200km in size and 5 km in high and whose effect has not been included in the POGM applied in this paper. G anomaly is a prominent magnetic anomaly that was interpreted by Rabinowiz and LaBreque (1979) as the boundary between oceanic and continental basement of the eastern Argentina; it was digitalized and drawn in red colour (Figure7a). It is interesting to observe in Figure 7a a high gradient of the variation of the crustal thickness limiting to the east with the 10 km contour and witch follows approximately the 3000 m

isobaths. We considered that this gradient points out a strong structural variation where the continental-oceanic boundary (COB) could be indicated. We analyzed that the transition zone should be considered to be between the 500m isobaths (this fits with the maximum of the free-edge effect anomaly) and the 3000m isobaths.

There is a circular characteristic zone in (44S, 58W)and it is noticeable that can be correlated with the same feature in the free-air gravity map (Figure 2) where a basin continuing in subsidence had been interpreted. This zone limits westward with the 10km contour and fits with the final track of the G anomaly northward to the Colorado discontinuity, and for this reason, this circular feature (strong pink colour) could be composed of oceanic crust.

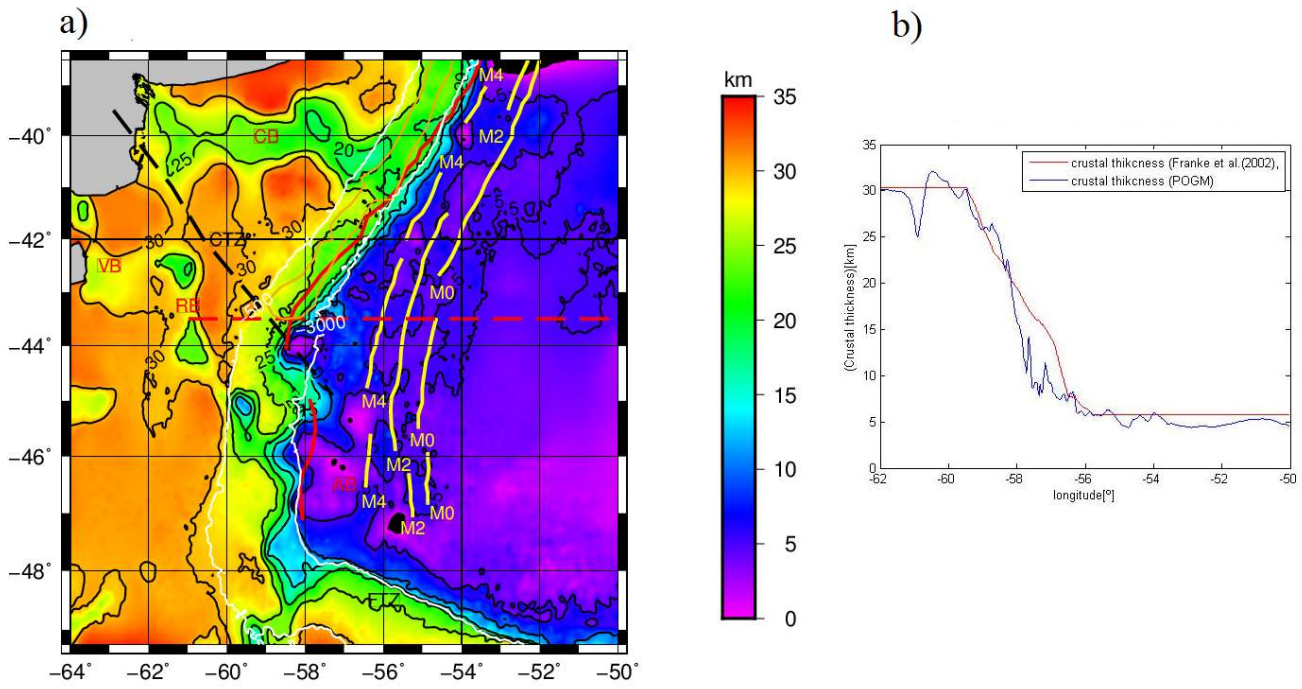

Figure 7: (a) 3D Crustal Thickness derived from POGM. The black dashed line corresponds to the Colorado transfer zone (CTZ). The 500 m and 3000 m isobaths are plotted in white line for reference. Mesozoic lineations are in yellow. The Colorado (CB), Rawson (RB), Valdés (VB) and Argentine (AB) basins are labelled in red. The red straight line corresponds to the G anomaly (Rabinowiz and Labreque, 1979.The red dashed line is the location of a seismic refraction profile (Franke et al, 2002).The orange straight line enclosures the main thick wedges of seaward dipping reflector sequences (SDRs) (Franke et al., 2007). (b) 2D Crustal Thickness from interfaces digitized from Franke et al. (2002) and the same profile from the POGM.

4.4 Calculating the rift anomaly (step 3.1, Figure 4)

A noticeable difference in details/resolution between Figure 9a and 9b is observed. Figure 9b is not a simple smoothing of the Figure 9a as we would have expected but it can have to do with a numerical effect.

Let us analyze Figure 9a in more detail: the free air anomaly at the time of rifting (i.e., considering settling as an independent event, not simultaneous with the rift) is represented. This is an approximation since the sediments have been considered as a single layer deposited after the rift event. A lineament that begins in the basins of Valdés and Rawson is observed and

continued in a third possible basin, which could be an abortive rift or aulacogen. This is evident from the palaeo-bathymetry maps (5a) and palaeo-Moho (5b) where it can be seen that the basin is being sustained by the mantle (what accounts for cortical shortening). The lineament could be interpreted as the union of a triple point between the abortive rift and the rift that resulted in the Atlantic.

4.5 Restoring sediment loading, flexure of the basement and the Moho (step 3.2, Figure 4)

The flexure of the basement is calculated and is applied to the Moho. The flexure can be seen in Figure 8, where a strong correlation with the sediment thickness scan be noticed (Figure 4), as we expected.

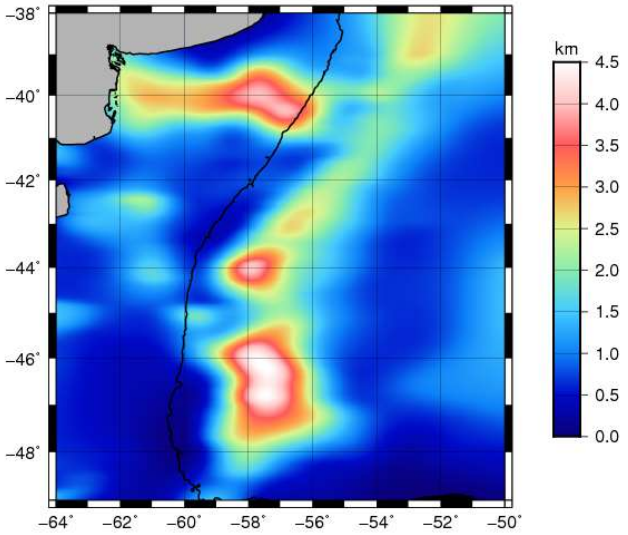

Figure 8: Flexure of the basement and the Moho. In both figures the 500 m isobath is plotted in black line for reference.

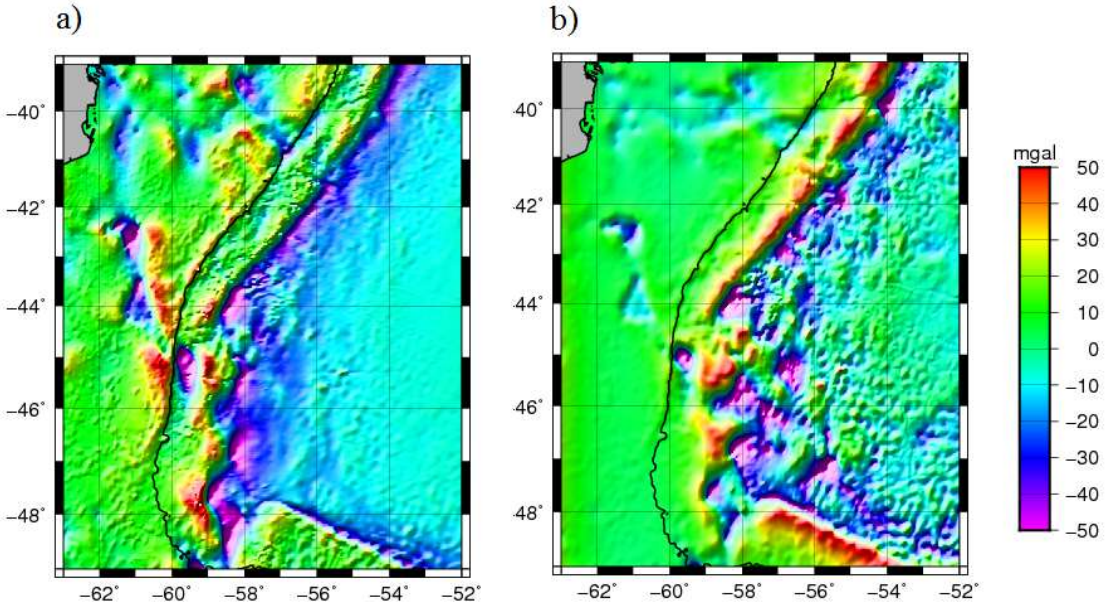

Figure 9: Rift anomaly from 2D (a) and from 3D (b). In both figures the 500 m isobath is plotted in black line for reference.

4.6Calculating the sedimentation anomaly (step 3.3, Figure 4)

Here the resolution in Figures 10a and 10b are maintained, since the calculation of the sediment anomaly is considered as a residual calculation. Regions in the sediment anomaly with a maximum indicate a maximum of the sedimentary thickness (Figure 3), where the load is located. The minimum defines regions where there is a displacement of the mantle with location of the crust in its replacement. In general, it has a maximum accompanied by two sidelobes, representing a symmetrical situation. Maxima with sharper minima than the other would be an asymmetric load situation.

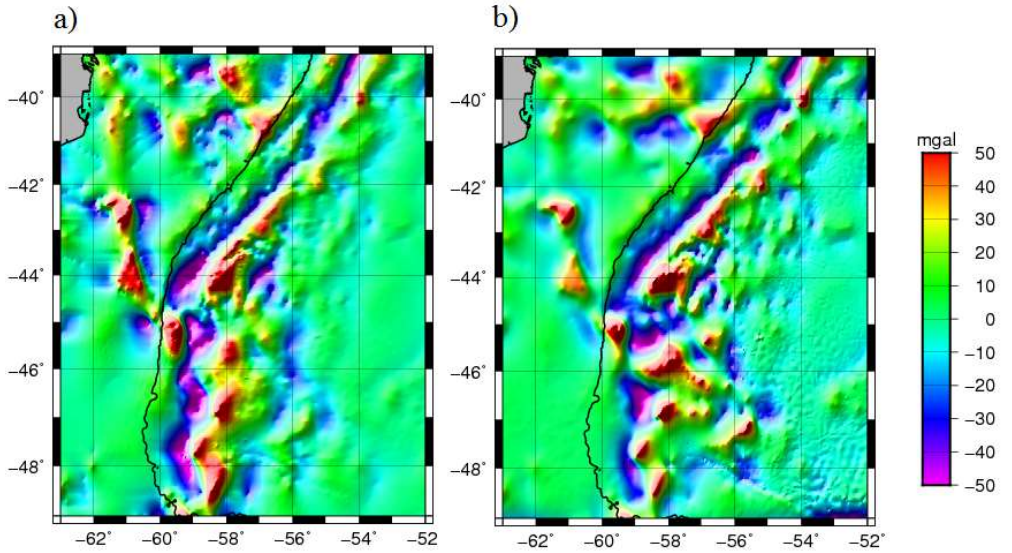

Figure 10: Sedimentation anomaly from 2D (a) and from 3D (b). In both figures the 500 m isobath is plotted in black line for reference.

4.7Obtaining the sum anomaly (step 3.4, Figure 4), comparing with the observed anomaly and constraining the Te values (step 4, Figure 4)

The sum anomaly calculated with the 2D approach (Figure 11a) displays the typical edge effect of the passive margins sharper than the 3D calculation (Figure 11b).There is a closer match with the edge effect present in the observed anomaly, so our 3D estimation is better achieved from the 2D profile approach. To constrain the T_e value the isostatic anomaly is minimized. Figure 10a shows the case where $T_e = 0\ km$ (according to Airy) and the Figure 12b shows the case for$T_e = 15\ km$. We note that $T_e = 15\ km$ best minimizes the isostatic anomaly (visual inspection) of several values ofT_e. The RMS between the observed anomaly and the sum anomaly is also minimal to this $T_e$as it is shown on Table2. The isostatic anomaly calculated by the flexural method and minimized for the case of $T_e = 15\ km$ can be compared with that obtained with the Airy method for which softened features are observed. It is noted that the flexural method obtains the minimum isostatic anomaly, with an elastic thickness of $15\ km$.For this reason, it is important to take into account the flexural model to improve the interpretation of gravity anomalies in marine zones.

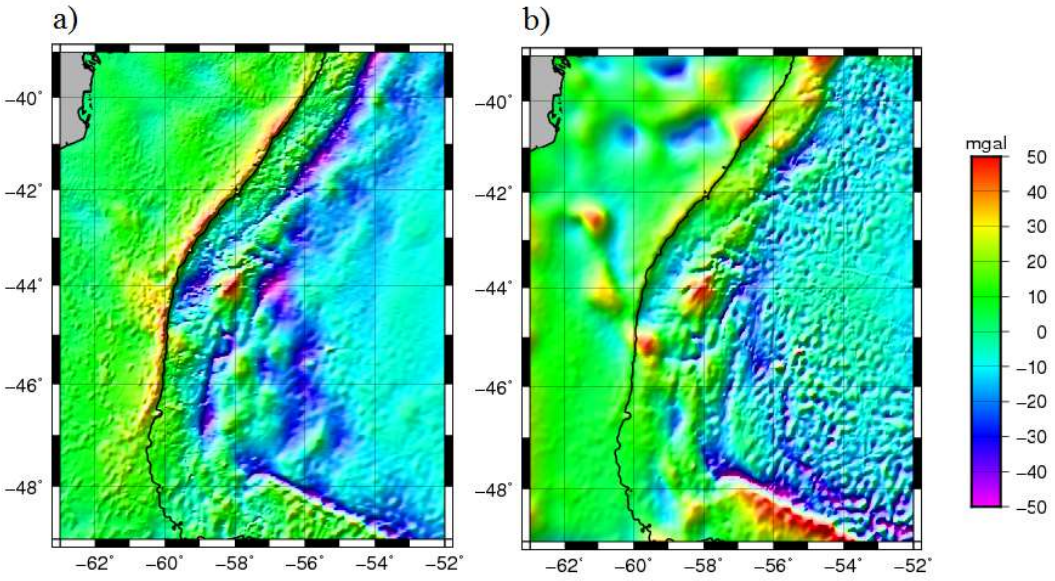

Figure 11: Sum anomaly from 2D (a) and from 3D (b). In both figures the 500 m isobath is plotted in black line for reference.

$T_e(km)$	$RMS(3D)$	$RMS(3D from\ 2D)$
0	17.13	-
5	16.94	12.43
10	16.32	12.06
15	15.89	11.85
20	16.21	12.42
25	17.31	-

Table 2: RMS of the POGM for grids with different values of effective elastic thickness (T_e).

Trough the analysis of the RMS minimum from different 2D profiles we conclude that a general decreasing tendency of the T_e toward the north exists, agreeing with the fact that the oceanic crust is younger, that is, the margin was opened from south to north (Rabinowitz et al., 1979). The numerical calculation is depend on the sedimentary grid used. So the minimum RMS criterion ought to be in agreement with a visual inspection of the behavior of the curves.

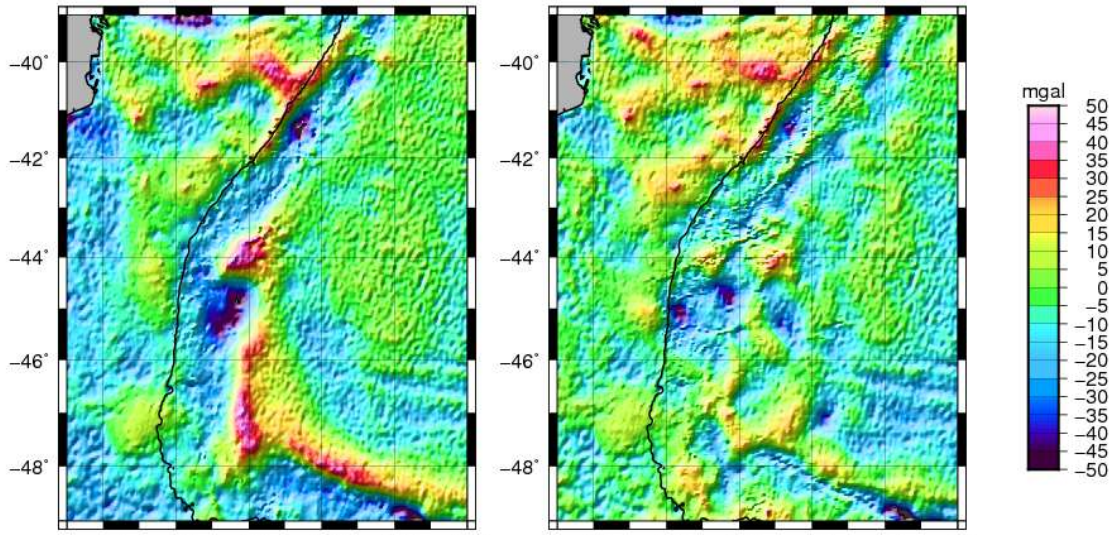

Figure 12: Isostatic anomaly according to Airy (a) and that calculated with POGM with Te=15km (b). In both figures the 500 m isobath is plotted as a black line for reference.

5Relationship with segmentation and with the geologic structures of the margin

On Figure 13 it is noteworthy that the grabens are enclosed by the double festoon to the free-air gravity edge effect and, immediately to the right, less marked the SRDs appear aligned in parallel. Figure13 also shows that the volcanic features of the margin changes towards the south and north of the Colorado discontinuity or the Colorado transfer zone. Figure 14also shows a graben to the right of the free-air gravity edge effect and then volcanic manifestations aligned with the abrupt change in gravity anomalies.

In Figure 15a, grabens are immersed in a negative value band; this band is attenuated slightly more in Figure 15b. In Figure 15a, a sudden change to north and south of the discontinuity of Colorado and a positive anomaly in Malvinas' transfer zone are observed, whereas in Figure 14b these features have been attenuated.

In Figures 12 and 15 volcanic spots appear in areas of gravimetric depressions, at least to the north of the Colorado discontinuity. It should be noted that in our approach we have not calculated the magmatic underplating effect which can exist associated with high-speed bodies as commonly detected by seismic lines under the SDRs.

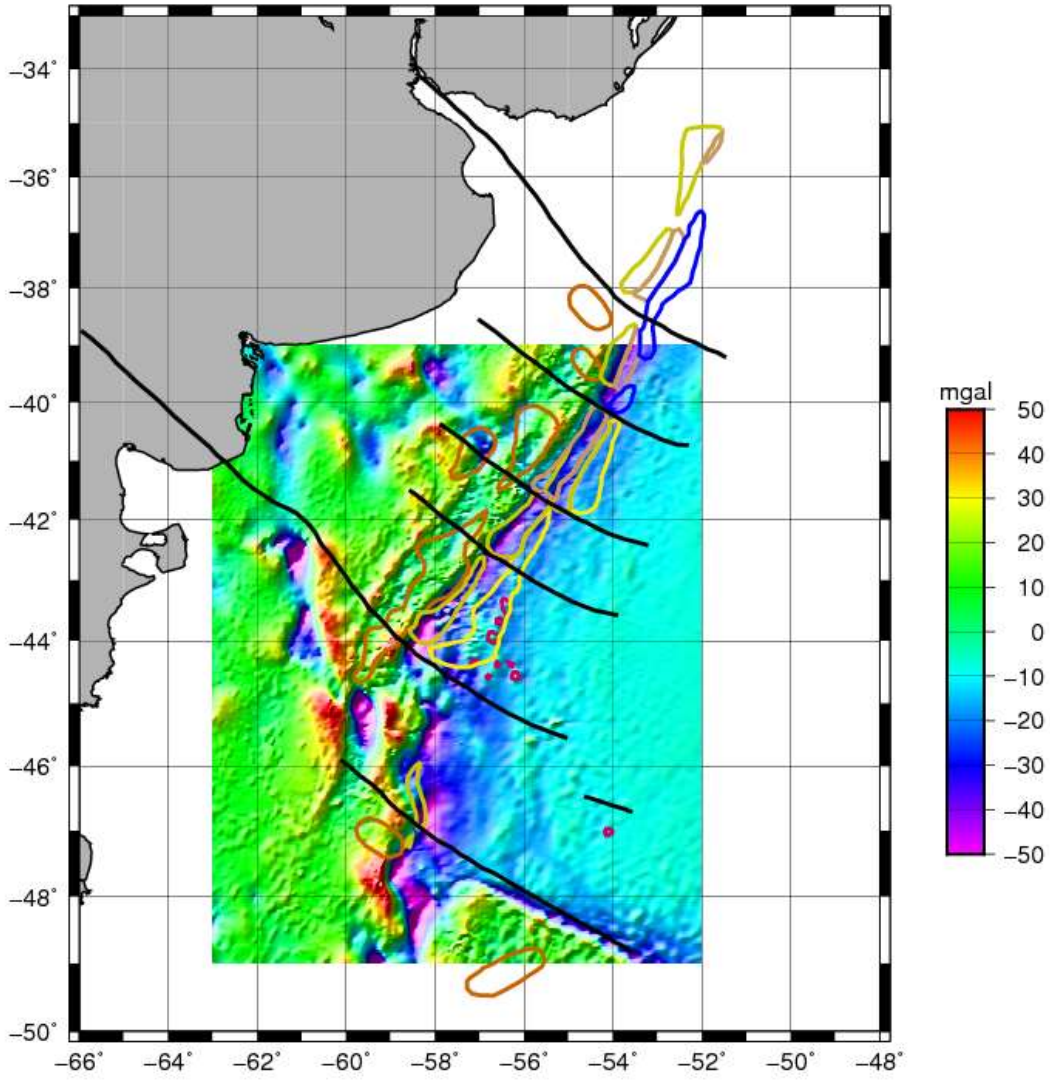

Figure 13: Rift anomaly from 2D and structures from the margin segmentation map have been superimposed. Dark brown lines represent pre/syn rift graben; black lines, transfer zones; fuchsia lines, intrusive; light green lines are SDRs wedges from episode1; light brown lines are wedges of the same episode 2; blue lines are depressions in the oceanic basement and yellow lines are basaltic lava flows (Franke et al., 2007).

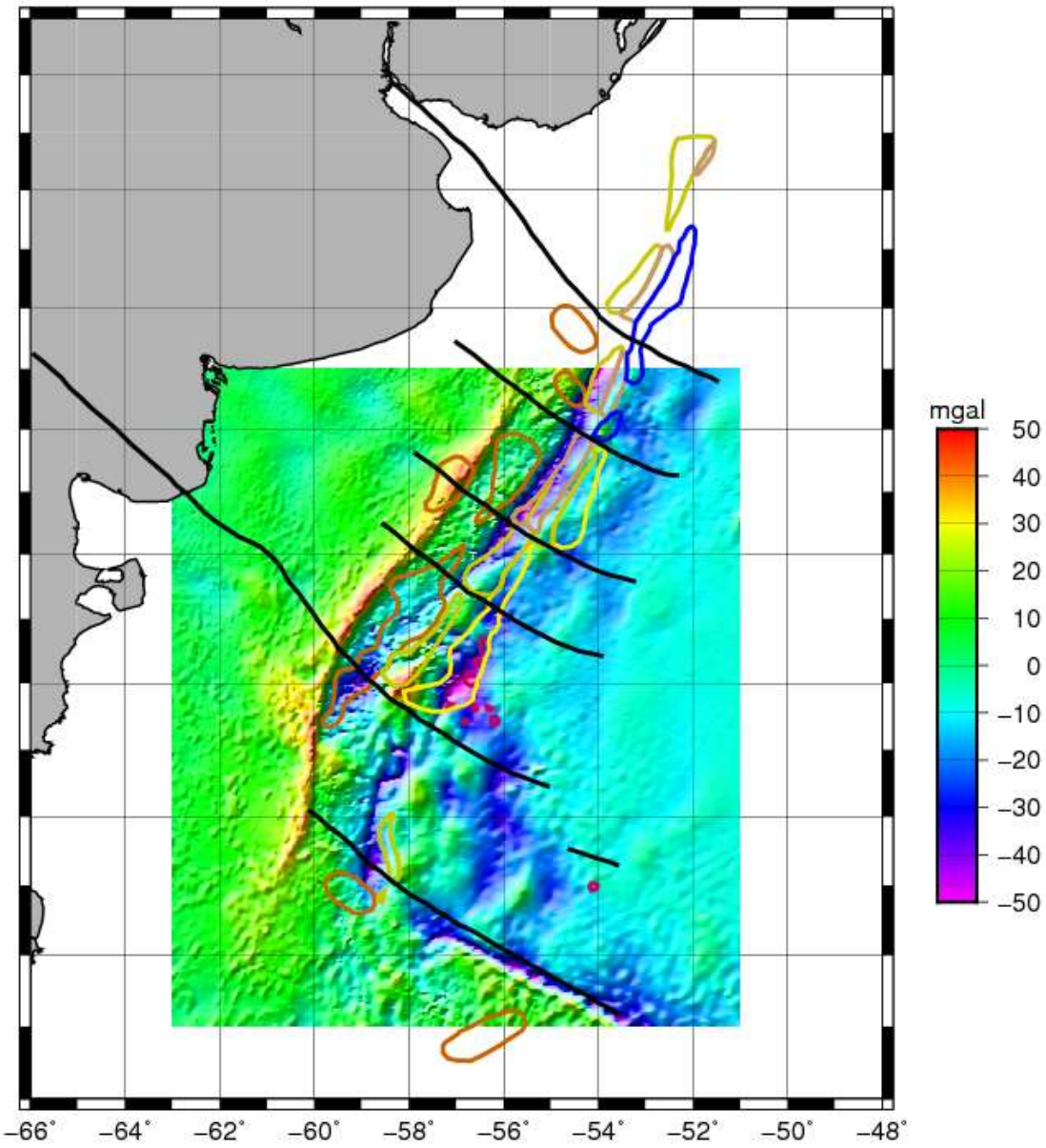

Figure 14: Sum anomaly from 2Dstructures from the margin segmentation map have been superimposed. Dark brown lines represent pre / syn rift graben, black lines transfer zones, fuchsia lines intrusive, light green lines are wedges of the same episode 1, light brown lines are wedges of the same episode 2, blue lines are depressions in the oceanic basement and yellow lines they are basaltic lava flows.

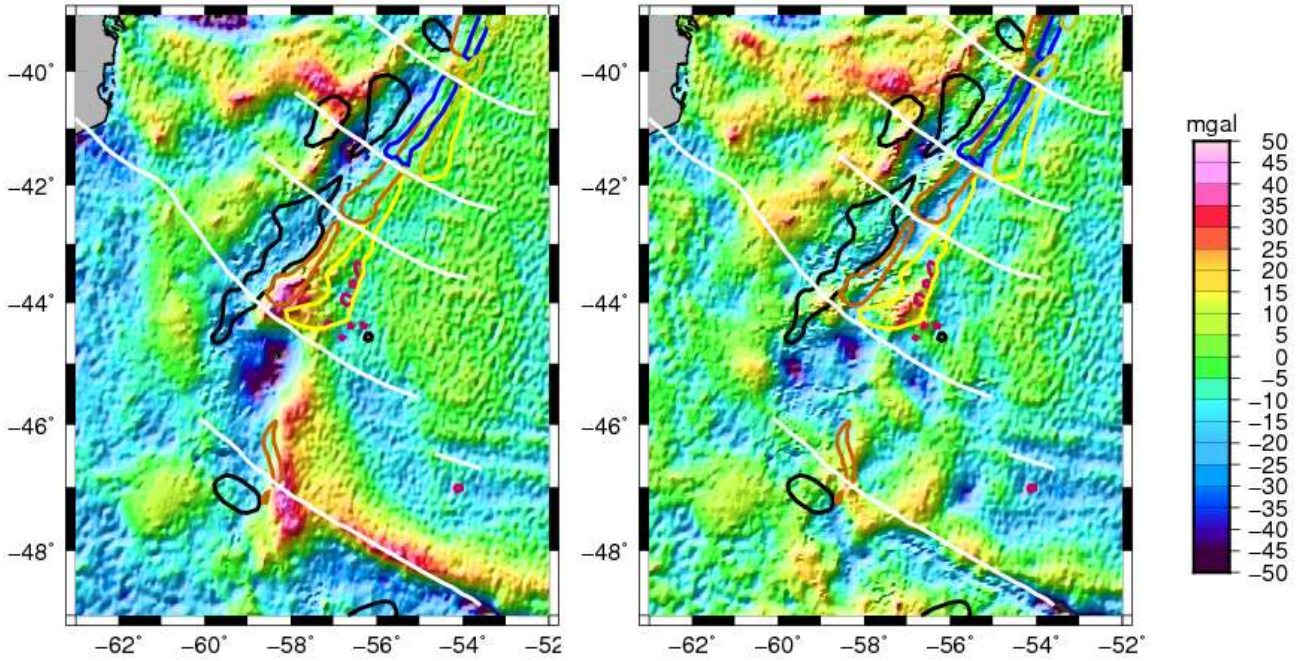

Figure 15: Isostatic anomaly according to Airy (a) and calculated with the POGM for Te = 15km, structures from the margin segmentation map have been superimposed. Black lines represent pre / syn rift graben; white lines transfer zones; intrusive fuchsia lines; dark brown lines are wedges of the same episode 1; light green lines are wedges of the same episode 2; blue lines are depressions in the oceanic basement and yellow lines are basaltic lavas flows.

6Discussion

In this work, the POGM methodology was applied to constrain the most representative T_e value of the area. This method minimises the isostatic anomaly and displays significant differences between the T_e structure of oceanic and continental lithosphere (Watts, 1999). Oceanic flexure studies suggest that T_e is in the range of 2–40 km and that it dependsonthe load and the plate age. On the other hand, T_e in the continents ranges from 0 to 100 km and shows no clear relationship with age (Burov and Watts, 2006). In the oceans, T_e is given approximately by the depth to the 450ºC isotherm in concordance with cooling plate models. For example, T_e increases from 4 to 12 km at the midoceanic ridge where the lithosphere is relatively young and hot to values greater than30 km where it is old and cold. Studies in the continents, however, do not show such a simple relationship between T_e and thermal age (Watts, 1999). It can be inferred that characterising the margin area, which is a zone where oceanic and continental crust are joined, with only one value of T_e is a first approximation to solve the current and old complex margin structure. In future works, we should develop or experiment with models that take into account different crusts as in Burov and Watts (2006).

7 Conclusions

POGM is the basis for an interpretation technique that allows us to distinguish the contribution that different geological processes make to gravity anomalies in marine areas. This gravity modelling is based on potential-field data where an inherent ambiguity is present in the results. However POGM has reduced it since theoretically it takes into account plausible schemes for the way that sediment and magmatism load the crust flexurally. This is the reason why we consider that flexural models cannot be "ignored" in gravity anomalies interpretation on passive margins.

Despite having worked with only one layer of sedimentary thickness with an average density and not having taken into account sea level changes and magmatic underplating effect, the implementation of the backstripping and POGM techniques on the Argentine continental margin represent an important contribution to isostatic studies and the current knowledge of the structure of the crust of the region.

As preliminary results of the 3D analysis, the following has been shown:

Basins are characterized by a thinned crustal thickness, which according to stretching factors analysis could show stretching periods did not reach the stage of oceanic crust formation. The location of a strong structural variation of crustal thickness can be associated with the COB.

The 3D approach from 2D is comparable to the 3D direct approach and it has more details in the platform zone, at the expense of a larger computational time.

An alignment in rift anomaly of Valdés and Rawson basin, which is continued on a possible third basin, could be an aborted rift or aulacogen. This can be seen on the crustal thickness map as evidence of a cortical shortening.

The isostatic anomaly shows a strong positive residue in the Colorado basin, which could suggest that the basin may continue in subsidence as pointed out by Introcaso et al. (1998).

The effect of magmatic underplating was not included in this work, but it is a challenge to incorporate its analysis in a 2D profile in a future work.

We need to improve the interpretation of the innovative anomalies derived from POGM also including a comprehensive analysis of other existing geophysical data with the aim to continue contributing to the complex issue evolution of the Argentine margin but unfortunately, we have not had access to them yet.

Acknowledgments

The global free air anomaly and bathymetry data used in this paper are of public domain and have been taken from http://topex.ucsd.edu/cgi-bin/get_data.cgi, 2011.

The maps have been plotted using the Generic Mapping Tools (GMT) free software (Wessel and Smith, 2007).

The authors thank Julián L. Gómez for his valuable help to improve the English version.

References

Andersen, O.B.; Knudsen P, 2010. Recent developments in high-resolution global altimetric gravity field modeling, The Leading Edge, v. 29, n.5, pp. 540-545.

Blaich, O.A., J.I. Faleide, F. Tsikalas, D. Franke and E. León, 2009.Crustal-scale architecture and segmentation of the Argentine margin and its conjugate off South Africa.Geophys. J. Int. (2009) 178, 85–105.

Burov E. B., 2006.The long-term strength of continental lithosphere: "jelly sandwelich" or "crème brûlée"?.Gsa Today. vol.16, no. 1, pp. 4-10.

Caminos R. and González, P. D., 1996. Mapa Geológico de la República Argentina. Publicación del Servicio Geológico Minero Argentino.

Coscia, C.A., 2000. Aprovechamiento de los datos sísmicos preexistentes para el análisis del espesor sedimentario en el margen continental argentino. En: Seminario de la Plataforma Continental, Buenos Aires, publicación del Consejo Argentino para las Relaciones Internacionales (CARI), pp. 249-265.

Cunha T., 2008. Gravity Anomalies, Flexure and the Thermo-Mechanical Evolution of the West Iberia Margin and its 30 Conjugate of Newfoundland. PhD Thesis, University of Oxford, Wolfson College & Department of Earth Sciences.

Eagles, G., M. Konig, 2008.A model of plate kinematics in Gondwana breakup.
20 Geophysical Journal International, 173, 703–717.

Eldholm, O., Skogseid, J., Planke, S. and Gladczenko, T.P. 1995. Volcanic margin concepts. In: Banda, E., Torné, M., Talwani, M. (Eds.), Rifted ocean–continent boundaries. Kluwer, Dordrecht, 1–16.

Franke, D., Neben, S., Hinz, K., Meyer, H. and Schreckenberger, B., 2002.Hidrocarbonhabitat of volcanic rifted passive margins.APG Hedberg conference.

Franke, D. ,Neben, S., Ladage, S., Schreckenberger, B., Hinz, K., 2007. Margin segmentation and volcano-tectonic architecture along the volcanic margin of Argentina/Uruguay, South Atlantic, Elsevier, Marine Geology, 244, 46-47.

Franke, D., 2013. Rifting, lithosphere breakup and volcanism: Comparison of magma-poor and volcanic rifted margins. Marine and Petroleum Geology, 43, 66-87.

Hayes, D.E. and LaBrecque, J.L., 1991. Sediment isopachs: Circum-Antarctic to 30°S. En: Marine Geological and Geophysical Atlas of the Circum-Antarctic to 30°S. Antarctic Research Series. Editadopor D.E. Hayes, AGU, Washington D.C., USA.

Hinz, K., S. Neben, B. Schreckenberger, H. A. Roeser, M. Block, K.G.D Souza y H. Meyer, 1999. The Argentine continental margin north of 48_S: sedimentary Successions, volcanic activity during breakup. Marine and Petroleum Geology 16, 1e25.

Hinze, W. J., Ralph R. B. von Frese , Afif H. Saad. 2013. Gravity and Magnetic Exploration. Cambridge University Press. ISBN: 978-0-521-87101-3.

Karner, G. D. and Watts, A. B. 1982.On isostasy at Atlantic-type continental margins. Journal of geophysical research, vol. 87, no. B4. pp. 2923-2948.

Introcaso, A. y Ramos, V. 1984. La cuenca del Salado. Un modelo de evolución aulacogénica. 9oCongresoGeológicoArgentino.Actas 3: 27-46.

Neben, A., Franke, D., Hinz, K., Schreckenberger, B., Meyer, H. and Roeser, H. A., 2002. Early Opening of the South Atlantic: Pre-Rift Extension and Episodicity of Seaward Dipping Reflector Sequence (SDRS), Emplacement on the Conjugate Argentine and Namibia Continental Margins. AAPG Hedberg Conference: Hydrocarbon Habitat of Volcanic Rifted Passive Margins. Stavanger, Noruega. Actas.

Nüremberg, D. and R. D. Müller, 1991.The tectonic evolution of the South Atlantic from Late Jurassic to present,Tectonophysics,191,pp. 27-53.

Moulin, M., Aslanian, D. and Unternehr, P., 2010. A new starting point for the South and Equatorial Atlantic Ocean, Earth-Science Reviews, 98, pp.1–37.

Parker C., Paterlini M. y Violante R. A., 1996. Compilación de datos sísmicos y determinación de isopacas en el Mar Argentino. Trabajo inédito, contribución al Mapa Geológico de la República Argentina.

Pedraza De Marchi A. C., Tocho C. y Ghidella M. 2012. Comparación de anomalías de gravedad derivadas de altimetría satelital con datos de gravedad marina en el margen continental argentino. Boletim de Ciencias Geodésicas, vol. 18, No. 1.

Pedraza De Marchi, A. C., 2015. Caracterización isostática del sector volcánico del margen continental argentino, Ph.D. thesis, Facultad de Ciencias Astronómicas y Geofísicas, Universidad Nacional de La Plata, 174 p.

Rabinowitz, P. D. and LaBrecque, J., 1979. The Mesozoic South Atlantic Ocean and evolution of its continental margins. Journal of Geophysical Research 84: 5973-6002.

Ramos, V. A., 1996. Evolución tectónica de la plataforma continental. En V. A. Ramos y M. A. Turic (Eds.) Geología y Recursos Naturales de la Plataforma Continental Argentina. XIII Congreso Geológico Argentino y III Congreso de Exploración de Hidrocarburos, Relatorio 21: 385-404.

Sandwell, D.T. and Smith, W. H. F, 1997. Marine Gravity from Geosat and ERS 1 Satellite Altimetry. J. Geophys. Res., vol. 102, no. B5, pp. 10039-10054.

Sandwell, D.T., Smith, W. H. F, Gille, S., Jayne, Steven, Soofi Khalid and Coakley, B., 20011994. Bathymetry from Space: White paper in support of a high-resolution, ocean altimeter mission, Sandwell2001BathymetryFS

Stewart, J., Watts, A. B. and Bagguley, J. G., 2000. Three-dimensional subsidence analysis and gravity modelling of the continental margin offshore Namibia. Geophys J. int., no. 141, pp. 724-746.

Szatmari, P., 2000. Habitat of petroleum along the South Atlantic margins. In: Mello, M.R., Katz, B.J. (Eds.), Petroleum Systems of South Atlantic Margins. AAPG Memoir, pp. 69e75.

Thorne, J. A. and A. B. Watts, 1989. Quantitative analysis of North Sea subsidence, The American Association of Petroleum Geologist Bulletin, 73, 1, pp. 88-116.

Watts, A. B. and Fairhead, J. D., 1999. A process-oriented approach to modeling the gravity signature of continental margins, The Leading Edge, no. 18, pp. 258-263.

Watts, A. B. & Ryan, W.B. F., 1976.Flexure of the lithosphere and continental margin basins, Tectonophysics, 36, pp. 25-44.

Watts, A. B. 1988. Gravity anomalies, crustal structure and flexure of the lithosphere at the Baltimore Canyon Trough. Earth and Planetary Sci. Lett., 89, pp. 221-238.

Watts, A. B. and Stewart, J., 1998. Gravity anomalies and segmentation of the continental margin offshore West Africa, Earth and Planetary Science Letters, no. 156, pp. 239-252.

Watts, A. B., 2001. Isostasy and Flexure of the Lithosphere, Cambridge University Press.

White R. and McKenzie, D., 1989. Magmatism at rift zones: The generation of volcanic continental margins and floods basalts, J. Geophys. Research, vol. 94, no. B6, pp. 7685-7729.

Zambrano, J. J., V. M. Urien, 1970. Geological outline of the basins in Southern Argentina and their continuation off the Atlantic Shore, J. Geophys. Research, 75, no 8.